# The Discovery of Velpatasvir (GS-5816): The Potent Pan-Genotypic Once-Daily Oral HCV NS5A Inhibitor in the Single-Tablet Regimens Epclusa® and Vosevi®

John O. Link

## Contents

**Abstract** The initial approval of the single-tablet regimen (STR) Harvoni®, containing the hepatitis C virus (HCV) nonstructural 5A protein (NS5A) inhibitor ledipasvir and the nonstructural 5B protein (NS5B) nucleotide inhibitor sofosbuvir (SOF), provided a major advancement in the treatment of individuals with chronic genotype 1 (GT1) HCV infection. Herein is described the discovery of velpatasvir (VEL, GS-5816), a pan-genotypic NS5A inhibitor with low picomolar activity against GT1–6 HCV and a high resistance barrier. The combinations of SOF/VEL as Epclusa® and SOF/VEL/voxilaprevir (VOX, NS3/4a protease inhibitor) as Vosevi® are the only pan-genotypic STRs for the treatment and cure of HCV infection. Epclusa® is the first approved pan-genotypic STR and affords high cure rates with a single 12-week treatment duration regardless of genotype, cirrhosis status, or the presence of baseline resistance variants. Vosevi® provides high cure rates for GT1–6-infected individuals who have previously failed therapy (96% cure rates for GT1–6 patients who had failed regimens with an NS5A inhibitor or 98% for those who had failed regimens without an NS5A inhibitor). With pan-genotype

J. O. Link (✉)
Medicinal Chemistry, Gilead Sciences, Foster City, CA, USA
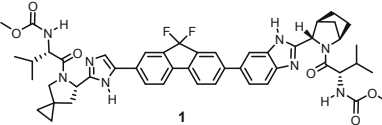e-mail: John.link@gilead.com

activity, no need for on-treatment monitoring, and real-world effectiveness comparable to that observed in clinical trials, the safe, simple, and effective STR Epclusa® is an important agent for eradication of HCV infection worldwide.

**Keywords** Direct-acting antiviral, Epclusa®, Vosevi®, GS-5816, HCV, NS5A inhibitor, Pan-genotypic, SOF/VEL, SOF/VEL/VOX, Velpatasvir
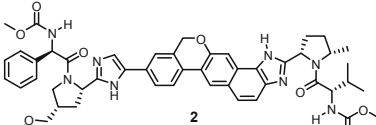
# 1 Introduction

Our initial work in nonstructural protein 5A (NS5A) inhibitor discovery led to ledipasvir (LDV, **1**, GS-5885, Table 1)[1] [2, 3]. LDV is the first NS5A inhibitor to be approved by the US Food and Drug Administration (FDA, October 10, 2014) and is combined with sofosbuvir in the single-tablet regimen (STR) Harvoni® [4–6].[2] The work toward LDV targeted the high unmet need for an effective treatment of HCV genotype 1 (GT1)-infected patients. This patient population had suffered high unmet need because (1) GT1 infection is the most prevalent worldwide among the six major HCV genotypes [7] and (2) among HCV genotypes, treatment of GT1 infection with the interferon (IFN)/ribavirin (RBV) standard of care resulted in lower sustained viral response (SVR, cure) rates [8–10]. As the first STR for HCV therapy, Harvoni provided a safe, simple, and effective treatment option for GT1 HCV-infected patients. The discovery work resulting in the high GT1 antiviral potency and long

**Table 1** Replicon cellular potency of ledipasvir and velpatasvir (GT1–6 replicons and subtypes) [1]



|       | GT EC$_{50}$ (pM) [1] | | | | | | | | | |
|-------|------|------|--------|---------|---------|---------|------|-----|-------|---------|
|       | 1a | 1b | 2aJFH1 | 2aJ6 | 2b | 3a | 4a | 5a | 6a | 6e |
| LDV   | 31 | 4 | 21,000 | 249,000 | 530,000 | 168,000 | 390 | 150 | 1,100 | 264,000 |
| VEL   | 14 | 16 | 8 | 16 | 6 | 4 | 9 | 54 | 6 | 130 |

[1]Unless otherwise noted, the EC50 values are based on the following replicon constructs for each genotype: 1a = GT1a (strain H77). 1b = GT1b Con-1. 2b = GT2b MD2b-1 NS5A. 3a = GT3a S52 transiently transfected subgenomic HCV replicon. 4a = GT4a ED43. 5a = GT5a SA13 NS5A (9-184) transient chimeric replicons based on GT1b Rluc backbone. 6a = GT6a HK6 stable subgenomic HCV replicon. In these replicons 1a, 1b, 2a, 3a and 4a are stable subgenomic replicon cells; 2aJ6 and 2b are NS5A transient chimeric replicons based on GT2a JFH-1 Rluc. backbone.
[2]https://www.accessdata.fda.gov/drugsatfda_docs/label/2015/205834s001lbl.pdf. Accessed 10 June 2018.

human pharmacokinetic half-life of LDV [2, 3, 6] (https://www.accessdata.fda.gov/drugsatfda_docs/label/2015/205834s001lbl.pdf. Accessed 10 June 2018) can be also be found in this volume of "HCV: The Journey from Discovery to a Cure."

After completing our research effort toward LDV, our next step was to discover an NS5A inhibitor with the potential to effectively treat all HCV-infected patients worldwide, regardless of genotype. The discovery of the pan-genotypic NS5A inhibitor velpatasvir (VEL, **2**, GS-5816, Table 1) described herein represents the culmination of these efforts [11, 12]. As guiding principles, we sought to discover an NS5A inhibitor with high potency across HCV genotypes 1–6, a low projected human dose, and once-daily pharmacokinetics sufficient for combination in an STR with one or more yet to be identified pan-genotypic agents of complementary antiviral mechanism. Although interferon (IFN) and ribavirin (RBV) treatment afforded higher SVR for GT2 and GT3 patients than for GT1 patients, the SVR was still far from optimal, and the therapy was complex and toxic leading many patients to defer treatment while their disease progressed to fibrosis and cirrhosis. Additionally, the real-world effectiveness (efficacy outside of a controlled clinical trial setting) of IFN-based therapies is far lower than reported clinical trial results arising from their complexity, toxicity, poor tolerability, and low efficacy [13]. As we envisioned with Harvoni for GT1 infection, we saw a parallel need for an STR for the treatment of GT1–6 HCV infection. STRs have been shown to improve patient compliance and concomitant efficacy in the chronic treatment of HIV infection [4, 5]. We envisioned that a single, simple, safe, and effective STR for HCV patients regardless of genotype would provide broad applicability for cure and ultimately eradication of HCV infection worldwide.

Toward this end, velpatasvir (100 mg) combined with sofosbuvir [14] (400 mg, Fig. 1) is the single-tablet regimen Epclusa®, a pan-genotypic and pan-cirrhotic 12-week treatment for HCV with overall cure rates of 98% [15–19] (https://www.gilead.com/~/media/files/pdfs/medicines/liver-disease/epclusa/epclusa_pi.pdf. Accessed 24 June 2018). The improvements in GT1–6 replicon potency for VEL over LDV are shown in Table 1. Further, the co-formulation of the pan-genotypic NS3/4a protease inhibitor voxilaprevir (100 mg, Fig. 1) with SOF and VEL is Vosevi®, an STR for the treatment of GT1–6 patients who have previously failed therapy with another regimen (96% SVR for GT1–6 patients who had failed with an NS5A inhibitor or 98% for those who had failed on a regimen without an NS5A inhibitor) [20, 21] (https://www.accessdata.fda.gov/drugsatfda_docs/label/2017/209195s000lbl.pdf. Accessed 10 June 2018). Epclusa® and Vosevi® are the only approved pan-genotypic STRs for the treatment of HCV infection.

## 2 Genetic Variability of the HCV Genome

The high mutability of HCV forms the basis for the chronicity of the virus [22]. It has been estimated that each possible single, double, and some triple viral mutants are produced daily within a single HCV-infected patient based on the high viral replication ($10^{12}$ viral particles produced daily) and the error-prone nature of the HCV

GS-7977, sofosbuvir (SOF)                    GS-9857, voxilaprevir (VOX)
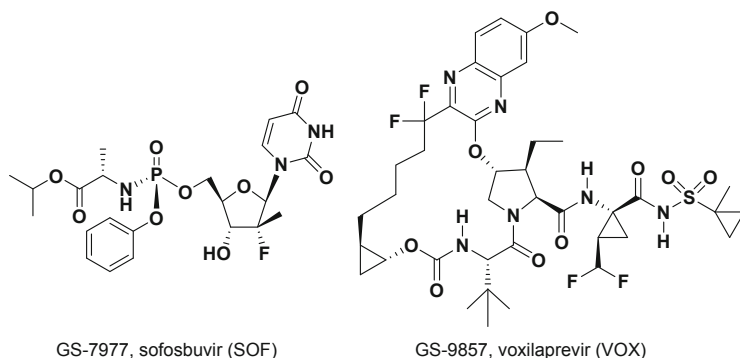
|               | SOF | LDV | VEL | VOX |      |
|---------------|-----|-----|-----|-----|------|
| Sovaldi®      | +   |     |     |     |      |
| Harvoni®      | +   | +   |     |     | STR  |
| Epclusa®      | +   |     | +   |     | STR  |
| Vosevi®       | +   |     | +   | +   | STR  |

**Fig. 1** Structures of sofosbuvir and voxilaprevir. Compositions of the single-tablet regimens (STRs) containing sofosbuvir

NS5B polymerase [23]. Further complicating the genetic landscape of HCV, there are eight known genotypes and 86 subtypes (another consequence of the high mutability of HCV) (https://talk.ictvonline.org/ictv_wikis/flaviviridae/w/sg_flavi/56/hcv-classification. Accessed 18 Dec 2018). Genotype prevalence is geographically heterogeneous. Of the six major genotypes (percent of worldwide infection noted in parentheses), GT1 (49%) is dominant in the USA, Asia, Japan, and Europe. GT2 (11%) and GT3 (18%) are prevalent in Europe and GT3 is dominant in India and Pakistan. Egypt, where GT4 (17%) is dominant, has the highest prevalence of HCV of any country worldwide at 8–15% of its population infected. GT4 is also prevalent in central Africa, and GT5 is almost exclusively found in South Africa. GT6 is found in Southern Asia. GT5 and GT6 infections total 5% worldwide [7]. There is high sequence variability in the coding region for the HCV NS5A protein, with many viral sequence variants arising from the high mutability of the virus in addition to the sequence variations among the genotypes and subtypes. This high variability presents a confounding challenge for discovering a pan-genotypic NS5A inhibitor. The viral sequence coding the NS5A region is among the most variable in the HCV genome; the basis for the variability in the NS5A region is unknown but may be derived from the finding that the NS5A protein has no known enzymatic activity [24] and therefore does not have an active site with typical obligate conserved residues. Many HCV variants have reduced susceptibility to inhibitors. The dominant sequence for each subtype is defined as the "wild-type" (WT) sequence, whereas variants that produce reduced susceptibility to inhibitors are defined as resistance-associated substitutions (RAS, plural RASs). These
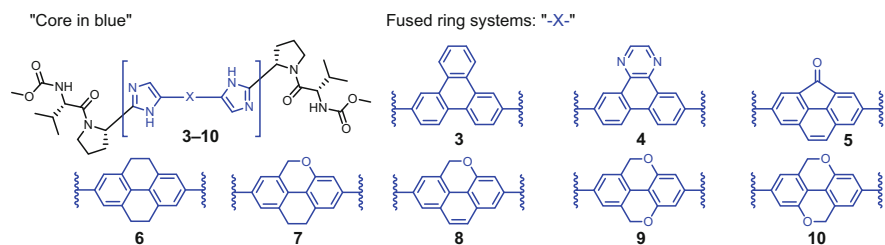
substitutions are annotated as "WT amino acid/residue position/substituted amino acid," e.g., Y93H (WT tyrosine at position 93 replaced by histidine). RASs in NS5A are commonly present at residue positions 28, 30, 31, 32, 58, 92, and 93 [25, 26]. Position 31 provides a useful example of the complexity of these substitutions: In GT1 L31 is WT, and L31M is a RAS. In GT2 L31M is a RAS that is more prevalent than in GT1 and is dominant in more than half of the GT2a and GT2b sequences. In GT4 M31 is present as WT and interestingly does not show reduced susceptibility to most inhibitors.

The structurally diverse set of NS5A proteins that would need to be potently inhibited by an effective pan-genotypic drug is daunting; similarly challenging is defining an assay paradigm representative of the viral species present in patients worldwide. To this end we analyzed patient-derived baseline (pre-treatment) NS5A gene sequences from public databases, along with sequences from our in-house clinical trial database to help understand the range of variation in the NS5A coding region. Central to our assay paradigm, we produced over 60 diverse and viable GT1–6 replicons to represent the diversity of HCV NS5A in infected individuals [1]. Consistent with published reports, we found that the prevalent GT2a and GT2b RAS L31M resulted in weaker potency against a range of NS5A inhibitor chemotypes [25, 26]. Additionally, subsequent to our discovery of VEL, it was reported that during monotherapy Phase 1 studies, an NS5A inhibitor produced a significantly weaker response in patients with GT2 L31M RAS present pre-treatment [27] (http://www.natap.org/2013/HCV/013113_03.htm. Accessed 14 Oct 2018).

Although we assayed for a range of genotypes and RASs, the structure-activity relationships (SAR) for inhibitor classes against GT2 L31M RASs provide instructive examples of our early studies to discover a pan-genotypic inhibitor (vide infra). We assayed for an increasing number of genotypes, subtypes, and RAS as our inhibitors evolved. Our inhibitors increased in structural complexity and size as we gained pan-genotypic activity; acceptable bioavailability and high metabolic stability proved increasingly difficult to obtain as our inhibitors gained broader activity against viral variants. High pan-genotypic potency, high metabolic stability, and good bioavailability were elements requiring significant parallel optimization to achieve our aim of discovering a pan-genotypic NS5A inhibitor with a sufficiently low dose for inclusion in an STR [11, 12, 28, 29].

## 3 Fused-Tetracyclic Core Inhibitors

Table 2 (see footnote 1) shows GT1 and GT2 replicon potency (potency values herein are reported as the effective concentration to inhibit replication in replicon cells by 50%, "$EC_{50}$") and predicted clearance (Pred CL) from human liver microsomes (HLM) for a number of inhibitors bearing fused tetracycle-based cores. Herein we define the "core" of the molecule as the moiety spanning between the C2 positions of the substituted pyrrolidines (core denoted in blue, Table 2). The GT2a JFH1 replicon in Table 1 is generated from a patient isolate derived clone

**Table 2** Cores with fused-ring systems provide high potency: replicon potency data and human liver microsomal metabolic stability values

"Core in blue"                          Fused ring systems: "-X-"



**3–10**

| | GT EC$_{50}$ (pM) | | | | | | |
|---|---|---|---|---|---|---|---|
| Cpd | 1a | 1b | 2a JFH1 (L31) | 2a JFH1-L31M[a] | 2a J6 (L31M) | 2b (L31M) | Pred CL (L/h/kg) HLM |
| 3 | 92 | 5 | 20 | 6,790 | – | – | <0.16[b] |
| 4 | 528 | 18 | 223 | – | – | – | <0.16 |
| 5 | 220 | 13 | 73 | – | – | – | 0.43 |
| 6 | 156 | 21 | 131 | 13,300 | – | – | 0.19 |
| 7 | 65 | 28 | 16 | – | 23,700 | – | 0.39 |
| 8 | 63 | 22 | 14 | – | 19,700 | 10,200 | 0.29 |
| 9 | 87 | 21 | 19 | 9,850 | – | – | – |
| 10[c] | 29 | 22 | 7 | 5,900 | 8,810 | 1,770 | 0.18 |

[a]GT2a JFH-1 subgenomic transient replicon cells with L31M mutation

[b]A value of <0.016 L/h/kg is the lowest predicted clearance value measurable in the routine HLM assay

[c]Additional replicon EC$_{50}$ values for compound **10**, GT(EC$_{50}$ value): 3a (GT3a S52 NS5A transient chimeric replicon based on GT1b Rluc backbone) (55 pM), 4a (GT4a ED43 NS5A transient chimeric replicons based on GT1b Rluc backbone) (29 pM), 5a (GT5a SA13 NS5A (9–184) transient chimeric replicons based on GT1b Rluc backbone) (56 pM), 6a (GT6a HK6 stable subgenomic HCV replicon) (16 pM), and 6e (GT6e D88 NS5A (9–184) transient chimeric replicons based on GT1b Rluc backbone. In these replicons a–c, g, and i are stable subgenomic replicon cells; d and f are NS5A transient chimeric replicons based on GT2a JFH-1 Rluc backbone) (1,160 pM)

bearing L31. Site-directed mutagenesis (SDM) was used to generate the GT2a JFH1-L31M replicon that served as our surrogate for the L31M RAS in early studies. Subsequently we utilized the patient-derived GT2a J6 and GT2b replicons that have L31M in their native sequence. We regard potency data against the L31M RAS from these patient-derived sequence replicons with greater weight than the surrogate JFH1-L31M; underlying sequence differences among these replicons are additional bases for their differing susceptibilities to inhibitors. We typically found that the GT2a J6 replicon was the most difficult to inhibit among these GT2 L31M replicons.

In our NS5A inhibitor program, we synthesized over 100 unique core systems with differing lengths, shapes, numbers of rings and ring topologies, flexibility or rigidity, degrees of saturation, and heteroatom count that were elaborated into full inhibitors [2, 3, 28, 29]. Throughout our studies one of the fruitful directions we undertook included utilization of fused-ring systems in the core of the inhibitor. As described in our discovery of ledipasvir, we found that fused-ring systems present in

the core of inhibitors could enhance GT1 potency [2, 6]. As we pursued pan-genotypic inhibitors, we found complex patterns of inhibition across genotypes where potency could sometimes be enhanced in certain inhibitors bearing fused-ring cores. We hypothesized that a highly evolved core structure could provide the base on which to build broad potency across genotypes.

Many of the complex core ring systems we designed were of unprecedented structure and were accessed through novel multistep synthetic paths. These core explorations required a significant resource commitment to chemical synthesis. To provide an example of such synthetic complexity, the route to the tetracyclic core inhibitor 7 is detailed in Scheme 1: Phenol **7a** was brominated with NBS, benzyl protected, and underwent Sonogoshira coupling with arylalkyne **7c**. Hydrogenation/hydrogenolysis of diarylalkyne **7c** and intramolecular biaryl coupling mediated by palladium acetate afforded dihydrophanthrene **7f**. Reduction with LAH afforded alcohol **7g** which was deprotected and cyclized to dihydronaphthochromene **7h** with boron tribromide. Triflation of 7h and formation of the boronate ester were followed by Suzuki coupling with bromo imidazole **7j**, followed again by boronate formation and Suzuki coupling with **7j** to complete the bis-imidazole dihydronaphthochromene core system (**7l**). Boc-deprotection of **7l** and HATU-mediated coupling with methoxycarbonyl valine gave tetracyclic pyran inhibitor **7** [11, 28, 29].

In our efforts to discover pan-genotypic inhibitors, we initially sought to enhance potency against the GT2 L31M RAS while maintaining high potency against the GT1a replicon. In one avenue we pursued a series of tetracyclic core inhibitors (Table 2) [11]. Relative to LDV, triphenylene core inhibitor **3** exhibits a ~threefold loss in GT1a potency along with a 1,050-fold gain in GT2a JFH1. Compound **3** was
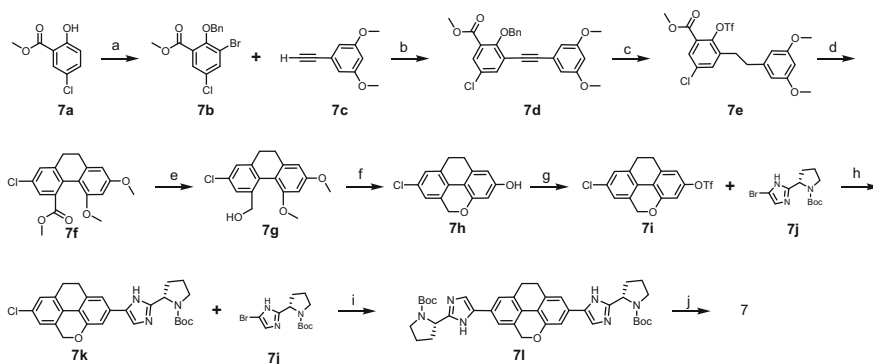


**Scheme 1** The synthesis of 7. (**a**) (i) N-bromosuccinimide, DMF (ii) BnBr, $K_2CO_3$, DMF. (**b**) Pd(PPh$_3$)$_4$, CuI, Et$_3$N, DMF, 80°C. (**c**) (i) H$_2$, Pd/C, 60 PSI, and (ii) Tf$_2$O, Py, CH$_2$Cl$_2$. (**d**) Pd(OAc)$_2$, PPh$_3$, Cy$_2$NMe, DMF, 110 °C. (**e**) LAH, THF. (**f**) BBr$_3$. (**g**) Tf$_2$O, Py, CH$_2$Cl$_2$. (**h**) (i) KOAc, Pd(dppf)Cl$_2$, (Bpin)$_2$, dioxane, 110 °C, and (ii) 7j, Pd(PPh$_3$)$_4$, K$_2$CO$_3$, DMSO, 100 °C. (**i**) (i) KOAc, Pd(dppf)Cl$_2$, X-Phos, (Bpin)$_2$, dioxane, 110 °C, and (ii) 7j, Pd(PPh$_3$)$_4$, K$_2$CO$_3$, DMSO, 100 °C. (**j**) (i) HCl, dioxane, CH$_2$Cl$_2$, and (ii) methoxycarbonyl valine, 1-[Bis (dimethylamino)methylene]-1*H*-1,2,3-triazolo[4,5-b]pyridinium 3-oxid hexafluorophosphate (HATU), i-Pr$_2$NEt

stable at the lower measurable limit of our HLM assay (Pred CL $< 0.16$ L/h/kg). The heterocyclic dibenzoquinoxaline system in **4** suffered losses in GT1a potency and GT2a JFH1 potency relative to the triphenylene inhibitor. We decided to change the tetracyclic ring topology. The cyclopentaphenanthrenone inhibitor **5** showed unacceptable losses in GT1 and GT2 activity. Again we changed the ring topology. Among the tetracycles **6–10**, incorporation of oxygen within the ring system proved beneficial. Proceeding from tetrahydropyrene **6** to tetracyclic pyran-based cores, **7** and **8** afforded enhanced GT1a and GT2 potency, although **6** proved more stable in HLM. Replacing the ethylene in **8** with methylenoxy afforded slight losses in GT1a and GT2a JFH1 potency. Importantly, the methylenoxy isomer **10** afforded the highest potency among the inhibitors in Table 2 for GT1a, GT2a JFH1, and the L31M GT2 variants. Although **10** had stability near the lower limit of our routine HLM assay (0.18 L/h/kg), improvements would need to be made to meet the criteria of once-daily dosing. Overall we considered the benzopyrano-benzopyran core system in **10** to provide the best balance of potency and stability within Table 2. Inhibitor **10** also showed potent activity against genotypes beyond GT1 and GT2: GT($EC_{50}$ value): 3a (55 pM), 4a (29 pM), 5a (56 pM), 6a (16 pM), and 6e (1,160 pM) (see footnote 1). The attributes of the core in benzopyrano-benzopyran inhibitor **10** warranted further study.

We investigated amino acid side-chain variants of inhibitor **10** (Table 3) (see footnote 1). Alkyl or cycloalkyl variants (**11–13**) showed losses in GT2a JFH1-L31M relative to valine. Intriguingly, the symmetric tetrahydropyranyl glycine (THP-Gly) inhibitor **14** displayed GT1a, GT2a J6, and GT2b $EC_{50}$ values that only varied by twofold (330–600 pM). The symmetric D-phenyl-glycine (D-PhGly) inhibitor **15** improved the profile further with $EC_{50}$ values of 93, 240, and 22 pM against GT1a, GT2a J6, and GT2b, respectively.

We became interested in understanding the pharmacokinetic properties of bis-D-PhGly inhibitor **15**. We have found that in high MW, low solubility, high lipophilicity "rulebreaker" [30] chemical space, some in vitro assay systems can produce artefactual results. This has been particularly true where systems have high surface area in the measurement apparatus – such as Caco2 permeability assays – potentially due to surface binding of the inhibitors. We have been unable to produce reliable Caco2 values for the inhibitors herein, including LDV and VEL. We prefer in vivo measurement of percent fraction absorbed ($F_a\%$) from non-precipitating solution dosing to gauge the permeability of these compounds. The calculation of fraction absorbed removes the hepatic clearance component from the measured bioavailability [bioavailability (F%) includes the percent fraction absorbed ($F_a\%$), hepatic clearance, and gut metabolism (herein our calculation of $F_a\%$ assumes no gut metabolism)]. We employ solution dosing from a non-precipitating formulation to remove the dissolution component from these pharmacokinetic studies. The calculation of $F_a\%$ removes the hepatic CL component of F% and therefore represents the gut absorption component [31]. The $F_a\%$ of bis-valine **10** and bis-D-PhGly **15** are shown in Table 4 in rat, dog, and cyno-monkey. The $F_a\%$ in dog for both compounds is moderate to high, but the values in rat and cyno tell a different story. The $F_a\%$ of compound **15** is exceedingly low in both rat and cyno (each are 2% $F_a$), while

**Table 3** Potency and metabolic stability derived from terminal amino acid modifications in benzypyrano-benzopyran series



11–18
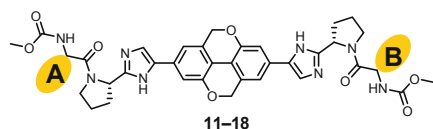
| Cpd | A | B | GT EC$_{50}$ (pM) | | | | | | Pred CL (L/h/kg) HLM |
|-----|---|---|------|------|------------|-------------------|-----------|-----------|-----------------------|
| | | | 1a | 1b | 2a JFH1 (L31) | 2a JFH1-L31M[a] | 2a J6 (M31) | 2b (M31) | |
| **11** | | | 31 | 19 | 9 | 12,100 | – | 1,850 | 0.18 |
| **12** | | | 53 | 20 | 20 | 31,300 | – | – | 0.21 |
| **13** | | | 55 | 22 | 22 | >44,000[b] | – | – | – |
| **14** | | | 380 | 800 | 74 | – | 330 | 600 | – |
| **15** | | | 93 | 48 | 7 | 145 | 240 | 22 | 0.19 |
| **16** | | | 185 | 172 | 14 | 1,330 | 1,430 | – | 0.23 |
| **17** | | | 87 | 79 | 10 | 3,670 | – | – | 0.21 |
| **18** | | | 50 | 31 | 4 | 600 | 1,820 | 76 | 0.24 |

[a]GT2a JFH-1 subgenomic transient replicon cells with L31M mutation
[b]Value of >44,000 means that the EC$_{50}$ was not achieved at this highest concentration tested

**Table 4** Fraction absorbed (F$_a$%) for benzopyrano-benzopyran series; bis-D-PhGly inhibitor 15 has low F$_a$% in rat and cyno

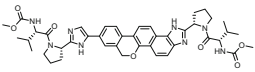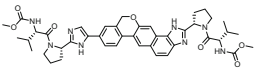| Cpd | Fraction absorbed (F$_a$%) | | |
|-----|-----|-----|-------------|
| | Rat | Dog | Cyno-monkey |
| 10 | 23 | 70 | 15 |
| 15 | 2 | 34 | 2 |

compound **10** shows moderate F$_a$% of 15–23%. It has been noted that drugs can undergo pericellular absorption in dogs due to the presence of "loose junctions" in their gut wall [32]. With our NS5A inhibitors, and other "rulebreaker" compounds, we have sometimes observed the trend of high F$_a$% in dog and low F$_a$% in rat and cyno. In these cases we therefore consider the high F$_a$% value for dog to be a species-specific value (for further examples, vide infra) and rely on rat and/or cyno values. Thus although compound **15** possesses important potency improvements, its low permeability presents a significant risk for progression. Since bis-valine compound

**10** afforded moderate $F_a$% in rat and cyno, and the bis-D-PhGly inhibitor possessed beneficial potency, we next pursued mixed amino acid inhibitors maintaining one valine in hopes of retaining permeability in inhibitors **16–18**. In this context, valine/D-PhGly inhibitor **18** produced a good potency profile that was intermediate between the profiles of symmetric inhibitors **10** and **15**. Although all compounds measured in the benzopyrano-benzopyran series in Table 2 had low Pred CL values in HLM, these values are not low enough to project to pharmacokinetic half-lives sufficient for once-daily dosing in humans since they range from 0.18 to 0.24 L/h/kg (the steady-state volumes of distribution [$V_{ss}$] for these compounds are typically 1–2 L/kg). We therefore sought to investigate further core discovery with the hope of improving human metabolic stability and further improve pan-genotypic potency.

## 4 Fused-Pentacyclic Inhibitors and the Discovery of Velpatasvir (VEL)

We decided to push further to even more complex fused-ring systems within the core of the inhibitors [11, 28, 29]. Pyranyl ring systems had proven beneficial (inhibitors **7–10**) so one design direction we undertook focused on the pyran-containing fused pentacyclic ring inhibitors **19** and **20** (Table 5, see footnote 1). We envisioned two alternate ring systems. In one system the methyleneoxy of the pyran is vicinal to the central ring of the embedded naphthimidazole (**19**) and an alternate ring system where the methylenoxy is distal to the middle ring of the embedded naphthimidazole (**20**). These unprecedented ring systems and a number of their precursors proved difficult to synthesize and isolate. As luck would have it, inhibitor **19** was synthesized and isolated first and presented a devastating setback for the team – where the significant effort required to produce this compound was met with potency and HLM stability results inferior to that of the tetracyclic benzopyrano-benzopyran **10**. Nonetheless we persevered with the synthesis and isolation of target **20**, and

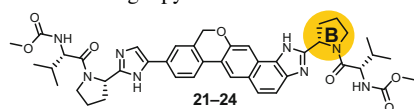**Table 5** Potency and metabolic stability of benzopyran-naphthimidazoles

| | | | GT EC$_{50}$ (pM) | | | | | | | Fraction abs. (F$_a$%) | |
| | Cpd | 1a | 1b | 2a JFH1 (L31) | 2a J6 (M31) | 2b (M31) | 3a | 4a | Pred CL (L/h/kg) HLM | Rat | Dog |
|---|---|---|---|---|---|---|---|---|---|---|---|
|  | **19** | 41 | 17 | 16 | 20,900 | 32,300 | 12 | 130 | 0.22 | 31 | 54 |
|  | **20** | 16 | 17 | 4 | 1,160 | 162 | 4 | 8 | <0.16 | 15 | 50 |

The metabolic stability and improved broad genotype potency of **20** is an important discovery

unexpectedly it showed a dramatic reversal in trend relative to its isomer **19**. *The core within inhibitor **20** contributes the greatest pan-genotype potency of any core system that we have synthesized.* For inhibitor **20** the replicon $EC_{50}$ values for GT1, 3 and 4 range from 4 to 17 pM, while the challenging GT2a J6 $EC_{50}$ is 1,160 pM and GT2b is 162 pM. The fold improvements for inhibitor **20** versus **19** are 18-fold for GT2a J6 and 199-fold for GT2b. Importantly, the pentacyclic benzopyrano-naphthimidazole **20** is stable within the conditions of the HLM assay (Pred CL < 0.16 L/h/kg), while the isomer **19** (along with the tetracyclic benzopyrano-benzopyran series) is less stable in HLM. The $F_a\%$ for **20** was 15% in rat showing potential for absorption. Interestingly, the pentacyclic benzopyrano-naphthimidazole would represent a new ring system in drug space; it has been noted that it is relatively rare to find newly applied ring systems in drugs [33]. We continued with investigation of inhibitors with the core system from pentacyclic benzopyrano-naphthimidazole **20**.

During our discovery of LDV, we found that modifications to the pyrrolidine rings could modulate GT1 potency and pharmacokinetic half-life [2, 3]. Thus in the pentacyclic benzopyrano-naphthimidazole core series, we pursued a number of pyrrolidine modifications, and important sets are represented in Tables 6 and 8.

**Table 6** Single pyrrolidine modifications in the benzopyran-naphthimidazole series



21–24

| B | Cpd | GT $EC_{50}$ (pM) | | | | | | | Pred CL (L/h/kg) HLM | Fraction absorbed ($F_a\%$) | | |
|---|---|---|---|---|---|---|---|---|---|---|---|---|
| | | 1a | 1b | 2a JFH1 | 2aJ6 (M31) | 2b (M31) | 3a[a] | 4a[b] | | Rat | Dog | Cyno |
| (pyrrolidine, 5) | 21[c] | 11 | 18 | 19 | 234 | – | 77[d] | 20[e] | – | – | – | – |
| (pyrrolidine, 4) | 22 | 11 | 18 | 7 | 443 | 132 | 18 | 11 | <0.16 | 10 | – | – |
| (pyrrolidine, O, 4) | 23 | 15 | 18 | 7 | 378 | 265 | 48 | 20 | <0.16 | – | – | – |
| (pyrrolidine, O, 4) | 24 | 21 | 26 | 8 | 280 | 135 | 24 | 14 | <0.16 | 16 | 56 | – |

[a]GT3a S52 NS5A transient chimeric replicon based on GT1b Rluc backbone
[b]GT4a ED43 NS5A transient chimeric replicons based on GT1b Rluc backbone
[c]The side chain of the valine on the methyl-pyrrolidine side is perdeutrated in compound **21**
[d]GT3a S52
[e]GT4a ED43

Table 6 (see footnote 1) shows a range of 4- and 5-position pyrrolidine substituents that each provides improved GT2a J6 potency relative to inhibitor **20** (**20** is unsubstituted at the 4- and 5-positions of the pyrrolidine). The 5-methyl inhibitor **21** afforded a GT2a J6 $EC_{50} = 234$ pM, although the GT3a potency eroded to 77 pM (relative to 4 pM in **20**). The 4-methyl inhibitor **22** was nearly as potent in GT 2a J6 (443 pM) as inhibitor **21** and had good GT3a potency at 18 pM. The 4-ethoxy inhibitor **23** had a relatively similar potency profile to that of the 4-methyl inhibitor. The 4-methoxymethyl substitution in inhibitor **24** improves on the 4-methyl and 4-ethoxy in GT2a J6 at 280 pM and is comparable to the 4-methyl inhibitor in GT3a affording the best overall potency profile we had yet seen. The 4-methoxymethyl emerged as an important pyrrolidine substituent. Importantly all inhibitors measured in HLM in the series are stable at the lower limit of the assay.

As has been apparent throughout the foregoing discussion, structural changes that improve potency against one genotype can lead to losses in potency against another. But as inhibitors trend toward improved potency across genotypes, we also noted that inhibitors can trend toward improved potency against RASs in various genotypes, although this remains a complex SAR. This trend is apparent in Table 7. We tested 4-methoxymethyl-substituted inhibitor **24** (best overall potency to this point) against clinically relevant GT1a RASs and show the results alongside those for LDV in Table 7. Inhibitor **24** displays improved potency against all GT1 RASs in Table 7 relative to LDV, with sub-nanomolar potency against most of these RASs. The complexity in the pattern of improvement is apparent from the observation that the fold improvement for each RAS from LDV to **24** is not constant and further that **24** *loses* potency relative to LDV versus GT1a and GT1b WT virus.

We continued with these modifications by pursuing substitutions on both pyrrolidines while keeping the beneficial 4-methoxymethyl substituent constant on pyrrolidine "B" for inhibitors **25**–**27** (Table 8, see footnote 1). Using 4-methoxymethyl substitution on both sides (**25**) drove the GT2a J6 potency to 61 pM (greatest potency for this subtype in Table 8) while being detrimental to GT3a potency (206 pM). Changing to the 4-methyl substituent lost some GT2a J6 potency (106 pM) while gaining GT3a potency (58 pM). Substitution of pyrrolidine "A" with a 5-methyl provided the best balance of potency in Table 8, with GT2a J6 and GT3a

**Table 7** Compound **24** has improved GT1 resistance profile

| | GT1a $EC_{50}$ (pM) | | | | | | | | GT1b $EC_{50}$ (pM) | |
|---|---|---|---|---|---|---|---|---|---|---|
| | WT | M28T | Q30H | Q30R | L31M | Y93C | Q30E | Y93H | WT | Y93H |
| LDV | 31 | 1,900 | 5,700 | 19,600 | 17,000 | 49,600 | 169,000 | 52,000 | 4 | 7,200 |
| 24 | 37 | 190 | 150 | 220 | 370 | 220 | 10,400 | 4,700 | 26 | 86 |
| Fold improvement of **24** over LDV | 0.84X | 10X | 38X | 89X | 46X | 225X | 16X | 11X | 0.15X | 84X |

All RAS are transiently transfected GT1a or GT1b subgenomic HCV replicons

**Table 8** Data for compounds with modifications to both pyrrolidines in the benzopyran-naphthimidazole series
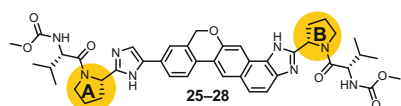


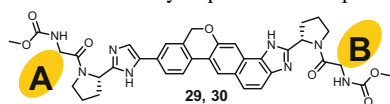| A | B | Cpd | GT EC$_{50}$ (pM) | | | | | | | Pred CL (L/h/kg) HLM | Fraction absorbed (F$_a$%) | | |
|---|---|---|---|---|---|---|---|---|---|---|---|---|---|
| | | | 1a | 1b | 2a JFH1 | 2aJ6 (M31) | 2b (M31) | 3a[a] | 4a[b] | | Rat | Dog | Cyno |
|  |  | **25** | 24 | 34 | 10 | 61 | 180 | 206 | 36 | <0.16 | 10 | – | – |
|  |  | **26** | 14 | 19 | 9 | 106 | 166 | 58 | 22 | <0.16 | 11 | – | – |
|  |  | **27** | 11 | 17 | 12 | 67 | 157 | 61 | 15 | <0.16 | 13 | – | 64 |
|  |  | **28** | 8 | 12 | 14 | 280 | 63 | 20 | 8 | <0.16 | 27 | 100 | 53 |

[a]GT3a S52 NS5A transient chimeric replicon based on GT1b Rluc backbone
[b]GT4a ED43 NS5A transient chimeric replicons based on GT1b Rluc backbone

nearly equipotent (67 and 61 pM, respectively), 11 pM GT1a activity, and GT2b potency at 157 pM. Assessing the 5-methyl substitution on both pyrrolidines (**28**) led to a less balanced profile than that of **27** with GT2a J6 potency at 280 pM. Thus the 4-methoxymethyl and 5-methyl work well in combination for potency. Notably, all compounds measured in Tables 6 and 8 have HLM Pred CL < 0.16 L/h/kg and low but double-digit F$_a$% in rat. Compounds **27** and **28** have good cyno F$_a$%.

Combining D-PhGly with valine in the benzopyrano-naphthimidazole series afforded inhibitors with potency below 134 pM (**29**) or 73 pM (**30**) for all genotypes tested (Table 9, see footnote 1). The concept (vide supra) that combining a valine on one side of the inhibitor with a D-PhGly on the other could provide a boost in permeability (relative to a bis-D-PhGly compound) is supported by the F$_a$% of 13% and 16% in rat and cyno, respectively, for inhibitor **29**.
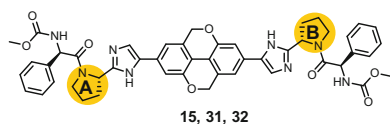
We sought to combine the beneficial pan-genotypic potency discoveries of the pyrrolidine substitutions with those of the D-PhGly. We approached this by determining if there was a matched or mismatched pairing of the 4- or 5-pyrrolidine with the D-PhGly. We pursued this in the symmetric tetracyclic benzopyrano-benzopyran inhibitor series in Table 10 (see footnote 1) for ease of synthesis. Indeed, the 5-methyl-pyrrolidine inhibitor provides a mismatch with the D-PhGly (less potent than the parallel unsubstituted pyrrolidine inhibitor **15** for the critical GT1a and

**Table 9** D-PhGly improves overall potency profile



**29, 30**

| A | B | Cpd | 1a | 1b | 2a JFH1 | 2aJ6 (M31) | 2b (M31) | 3a[a] | 4a[b] | Pred CL (L/h/kg) HLM | Rat | Dog | Cyno |
|---|---|---|----|----|---------|------------|----------|-------|-------|----------------------|-----|-----|------|
| | | | | | | | | | | | Fraction absorbed (F$_a$%) | | |
| | | | **GT EC$_{50}$ (pM)** | | | | | | | | | | |
| | | **29** | 22 | 21 | 4 | 134 | 12 | 5 | 8 | <0.16 | 13 | 56 | 16 |
| | | **30** | 35 | 33 | 6 | 73 | 16 | 6 | 11 | <0.16 | – | – | – |

[a]GT3a S52 NS5A transient chimeric replicon based on GT1b Rluc backbone
[b]GT4a ED43 NS5A transient chimeric replicons based on GT1b Rluc backbone

**Table 10** 5-Methyl-pyrrolidine generally antagonizes, and 4-methyl-pyrrolidine generally synergizes, with D-PhGly relative to the des-methyl-pyrrolidine inhibitor **15**



**15, 31, 32**

| A | B | Cpd | 1a | 1b | 2a JFH1 | 2aJ6 (M31) | 2b (M31) | 3a[a] | 4a[b] | Pred CL (L/h/kg) HLM | Rat | Dog |
|---|---|---|----|----|---------|------------|----------|-------|-------|----------------------|-----|-----|
| | | | | | | | | | | | Fraction absorbed (F$_a$%) | |
| | | | **GT EC$_{50}$ (pM)** | | | | | | | | | |
| | | **15** | 93 | 48 | 7 | 240 | 22 | – | – | 0.19 | 2 | 34 |
| | | **31** | 150 | 20 | 8 | 1,835 | 94 | 4 | 15 | <0.16 | 3 | 43 |
| | | **32** | 31 | 20 | 5 | 58 | 26 | 6 | 13 | <0.16 | 2 | 30 |

[a]GT3a S52 NS5A transient chimeric replicon based on GT1b Rluc backbone
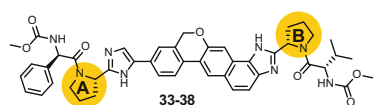[b]GT4a ED43 NS5A transient chimeric replicons based on GT1b Rluc backbone

GT2a J6). In contrast, the 4-methyl-pyrrolidine **32** provides a matched pair with the D-PhGly and is similar or improved in potency against all genotypes relative to **15**, with GT1a and GT2a J6 showing threefold and fourfold improvements, respectively. Again, like inhibitor **15**, these bis-D-PhGly inhibitors **31** and **32** have very low F$_a$% in rat (3 and 2%, respectively) and the apparently species-specific high permeability

in dog. Thus despite the excellent pan-genotypic potency of inhibitor **32**, its low permeability renders it a high risk for development.

We intended to exploit the finding of potency synergy between 4-pyrrolidine substitution and D-PhGly (Table 10) in the pentacyclic benzopyrano-naphthimidazole series (Table 11, see footnote 1). Indeed combination of the 4-methoxymethyl-pyrrolidine with the D-PhGly in inhibitor **33** provided our most potent pan-genotypic inhibitor to this point, with potencies for all genotypes ≤19 pM. Unfortunately the $F_a$% for this inhibitor is low in rat (12%) and very low in cyno (3%). Contrary to prevailing thought, we have found that small structural changes in "rulebreaker" chemical space (changes that make no significant change in the rule-based calculated metric values) can provide significant shifts in measured

**Table 11** Pyrrolidine "B" modification improves potency and fraction absorbed resulting in velpatasvir (**2**)



| A | B | Cpd | 1a | 1b | 2aJFH1 | 2aJ6 (M31) | 2b | 3a[a] | 4a[b] | Pred CL (L/h/kg) HLM | Rat | Dog | Cyno |
|---|---|---|---|---|---|---|---|---|---|---|---|---|---|
| | | | | | GT EC50 (pM) | | | | | | Fraction absorbed (Fa%) | | |
| | | **33** | 11 | 19 | 6 | 13 | 9 | 17 | 7 | <0.16 | 12 | – | 3 |
| | | **34** | 13 | 17 | 6 | 14 | 15 | 25 | 11 | <0.16 | 9 | – | 4 |
| | | **35** | 10 | 11 | 6 | 113 | 46 | 18 | 9 | 0.24 | – | – | – |
| | | **36** | 13 | 20 | 7 | 21 | 28 | 25 | 9 | <0.16 | 13 | – | – |
| | | **2 VEL** | 14 | 16 | 8 | 16 | 6 | 4[c] | 9 | <0.16 | 36 | 29 | 37 |
| | | **37** | 8 | 5 | 4 | 53 | 15 | 20 | | <0.16 | 4 | – | – |
| | | **38** | 33 | 30 | 18 | 45 | 27 | 50 | 63 | <0.16 | 4 | – | – |

[a]GT3a S52 NS5A transient chimeric replicon based on GT1b Rluc backbone
[b]GT4a ED43
[c]GT3a S52 transiently transfected subgenomic HCV replicon

pharmacokinetic parameters (such as fraction absorbed or bioavailability). Thus we held the matched pairing of methoxymethyl and D-PhGly constant while making modifications to the pyrrolidine "B" seeking to improve the $F_a$%. Substitution with 4-methyl in (**34**) did not provide $F_a$% improvement, and cyclopropyl ring fusions (which can be considered an interpolation of the 4- and 5-methyl substitution in isomers **35** and **36**) resulted in a loss of GT2a J6 potency in **35** and no benefit in $F_a$% in **36**. Strikingly, moving to a 5-methyl substitution in inhibitor **2** resulted in a positive frameshift in $F_a$% in both rat and cyno to 36 and 37%, respectively. Further inhibitor **2** maintained high pan-genotypic activity at $\leq 16$ pM for the genotypes detailed in Table 11. This standout inhibitor **2** was selected for development and is now known as velpatasvir [11, 12, 28, 29].

Further close analogs are inferior to VEL; **37** (where the 4-methoxymethyl of VEL is replaced by methyl) and **38,** which is the isomer of **37,** display low fractions absorbed in rat (4%). Continuing with the theme of variations related to VEL, the inhibitor where the pentacyclic benzopyrano-naphthimidazole of VEL is "swapped" for the tetracyclic benzopyrano-benzopyran imidazole-based core (compound **39**, Table 12, see footnote 1) was synthesized and tested. Although **39** displays the most advanced overall potency and PK profile in the tetracyclic benzopyrano-benzopyran series, it falls short of VEL in potency for GT2 and GT3, HLM stability, and $F_a$% in rat. Other inhibitors with similar structures to VEL (depicted in Fig. 2) were synthesized and also have inferior characteristics: The dihydro analog **40** has threefold higher HLM Pred CL, the oxo inhibitor **41** loses 2- to 12-fold in potency across GT1–4, and "flipping" the core results in compound **42** that has a 13% $F_a$% in rat (Fig. 2).

**Table 12** Replacing the benzopyrano-naphthimidazole core of VEL with the benzopyrano-benzopyran core results in an inferior profile



Compound 39
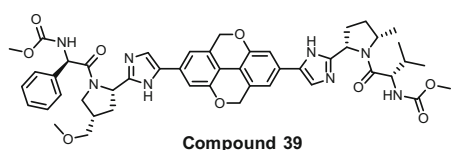
| GT EC$_{50}$ (pM) | | | | | | | | | Pred CL (L/h/kg) HLM | Fraction abs. (F$_a$%) | |
|---|---|---|---|---|---|---|---|---|---|---|---|
| 1a | 1b | 2aJ6 | 2b | 3a[a] | 4a[b] | 5a | 6a | 6e | | Rat | Monkey |
| 16 | 16 | 480 | 290 | 120 | 13 | 81 | 22 | 110 | 0.20 | 29 | 26 |

[a]GT3a S52 NS5A transient chimeric replicon based on GT1b Rluc backbone
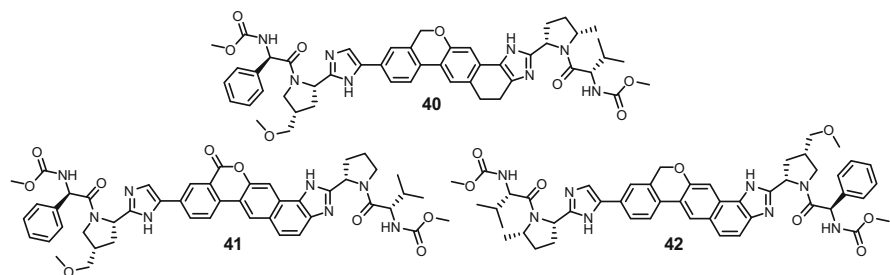[b]GT4a ED43

**Fig. 2** Comparator structures to velpatasvir

## 5 Velpatasvir Synthesis

A synthesis of velpatasvir and the intermediate Boc-4-methoxymethylproline (**43**) are outlined in Schemes 2 and 3 [12, 28, 29]. Treatment of phenol **2b** with benzylic chloride **2a** under basic conditions forms ether **2c**, which undergoes palladium-mediated biaryl coupling to form tetracyclic ketone **2d**. Vinylation of **2d** forms styrene **2e** which is converted to the bromohydrin **2f** with NBS under hydrolytic conditions. The bromoketone **2g** resulting from oxidation of **2f** is used to alkylate the acid of Boc-protected methoxymethylproline **43** to form ester **2h**. Bromoketone **2i** results from bromination of **2h** and is then alkylated with dipeptide acid **44** to form diketo-diester **2j**. Heating **2j** in the presence of ammonium acetate effects double imidazole formation to form the fused pentacycle in **2k**. Oxidation completes the
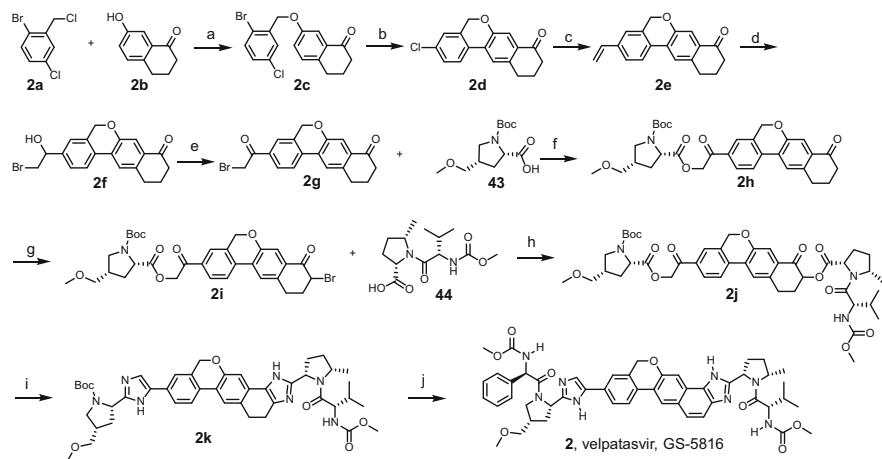


**Scheme 2** Synthesis of VEL. (**a**) $K_2CO_3$, DMAc. (**b**) $Pd_2(dba)_3$, P(4-F-Ph)$_3$, PivOH, $K_2CO_3$. (**c**) $CH_2CH_2BF_3K$, Pd(OAc)$_2$, S-Phos, n-PrOH. (**d**) NBS, THF/DMSO/$H_2O$. (**e**) $MnO_2$, $CH_2Cl_2$. (**f**) **43**, $K_2CO_3$, $CH_2Cl_2$. (**g**) PyHBr$_3$, $CH_2Cl_2$, MeOH. (**h**) **44**, $Cs_2CO_3$, MeTHF. (**i**) $NH_4OAc$, toluene, 2-methoxyethanol. (**j**) (i) $MnO_2$, $CH_2Cl_2$ (ii) HCl, dioxane, $CH_2Cl_2$, and (iii) methoxycarbonyl-D-phenylglycine, COMU, i-Pr$_2$NEt, DMF
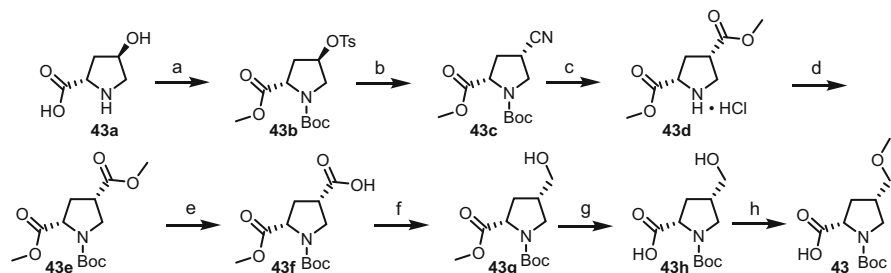
**Scheme 3** Synthesis of Boc-methoxymethylproline. (**a**) (i) SOCl$_2$, CH$_2$Cl$_2$, (ii) Boc$_2$O, NaHCO$_3$, CH$_2$Cl$_2$, H$_2$O, and (iii) TosCl, Et$_3$N, DMAP, CH$_2$Cl$_2$. (**b**) NaCN, DMSO. (**c**) AcCl, MeOH. (**d**) Boc$_2$O, NaHCO$_3$, EtOAc, H$_2$O. (**e**) NaOH, MeOH. (**f**) BH$_3$•THF, MeTHF. (**g**) NaOH, MTBE. (**h**) MeI, NaOtBu, THF

elaborated core, and Boc-deprotection followed by coupling with methoxycarbonyl-D-phenylglycine provides velpatasvir (**2**).

Boc-protected methoxymethylproline (**43**) is synthesized starting with hydroxy-proline (**43a**) (Scheme 3). Esterification, Boc-protection, and tosylation provide **43b**. Tosylate displacement forms cyano-proline **43c,** and its treatment with methanolic HCl effects cyano conversion to the methyl ester along with Boc-deprotection (**43d**). Reprotection and selective ester hydrolysis provide acid **43f** which is reduced with borane to alcohol **43g**. Ester hydrolysis and alcohol methylation afford Boc-protected methoxymethylproline (**43**).

Our commitment of extensive resources to the discovery of new cores was a fundamental aspect of our NS5A program. It has been posited that chemists resort to known ring systems due to the chemical synthesis resource cost of novel ring systems [34]. The pentacyclic benzopyrano-naphthimidizole is a novel ring system, and its discovery, despite its chemical and synthetic complexity, proved important.

# 6 Velpatasvir Nonclinical Data and Clinical Antiviral Activity

In vitro protein binding and metabolism and in vivo pharmacokinetic parameters for VEL are shown in Table 13. VEL is highly protein-bound with 0.2–0.4% free drug in rat, dog, and monkey plasma; the human plasma value is intermediate in this range at 0.3% free. The predicted clearance from microsomes is low across nonclinical species, and the values are similar to the clearance observed in vivo, suggesting that the main route of clearance is hepatic oxidative metabolism. Since VEL did not show measurable instability in our routine HLM assay (Table 11, Pred CL < 0.16 L/h/kg), $^3$H-VEL was assayed in human hepatocytes with quantitation of metabolites. This method affords accurate measurement of metabolism at lower levels than in the routine assay and resulted in a low Pred CL for VEL of 0.06 L/h/kg. In rat, dog, and

**Table 13** VEL in vitro protein binding and metabolism and in vivo PK parameters in preclinical species and healthy volunteers

| | | In vitro | | In vivo | | | |
| | Dose (route) | % Free plasma | Pred CL microsomes (L/h/kg) | CL (L/h/kg) | $V_{ss}$ (L/kg) | $t_{1/2}$ (h) | F% |
|---|---|---|---|---|---|---|---|
| Rat | (IV) | 0.2 | 0.74 | 0.94 | 1.61 | 2.25 | 28 |
| Dog | (IV) | 0.2 | 0.37 | 0.25 | 1.43 | 5.20 | 25 |
| Monkey | (IV) | 0.4 | <0.17 | 0.30 | 1.60 | 5.03 | 30 |
| Human | 100 mg (PO) | 0.3 | 0.06[a] | – | – | 15.7 | ~50[b] |

[a]Data generated in hepatocytes using ^{3}H-VEL
[b]Calculated from human oral CL/F and human predicted clearance from nonclinical data

cyno, the steady-state volumes of distribution ($V_{ss}$) are higher than total body water and range from 1.4 to 1.6 L/kg. Half-lives and bioavailabilities range from 2.2 to 5.2 h and 25–30%, respectively [11]. Taken together the nonclinical data are consistent with the potential for VEL to be dosed once-daily with low clearance and low dose in human and were the basis for the progression of VEL into clinical studies.

Gratifyingly the human half-life of VEL is 15.7 h at the 100 mg dose used in Epclusa®, consistent with once-daily dosing (Table 13) [35]. Estimation of the human bioavailability from the clinical solid dosage form is 50% and exceeds the solution-dosed bioavailability values in rat, dog, and cyno. The plasma exposure curves after three oral doses in healthy volunteers are shown in Fig. 3. The concentration of VEL at 24 h post the third dose exceeds its GT1–6 average protein adjusted EC$_{50}$ at all dose levels from 5 to 450 mg total dose (dotted line, Fig. 3).

Sets of rules seeking to predict orally bioavailable and "drug-likeness" chemical space have proliferated in the medicinal chemistry literature since the seminal 1996 publication by Lipinski on the "Rule of 5" [36]. Rule-based dogma now pervades the medicinal chemistry literature. A subset of such rules is noted in Table 14, along with the "rule limit value" and the values calculated for LDV and VEL. These rule-based approaches typically define a count or calculation and then set limit values at 90th or 95th percentile of known oral drugs falling below the limit. LDV and VEL are "rulebreakers" [30], violating three-out-of-four of Lipinski's Rule of 5 (two violations are needed to "break" the Rule of 5) and breaking each of Veber's rotatable bond and polar surface area rules [37, 38], the number of aromatic ring rule [38], and the number of total ring rules [33]. Both LDV and VEL values fall significantly beyond the majority of the rule limit values. The values in Table 14 are provided for reference and discussion; we did not calculate, consider, nor abide by these limiting rule-based concepts in the discovery of the orally bioavailable inhibitors LDV or VEL. Instead, as discussed herein, we utilized in vitro and in vivo data along with hypothesis generation and testing to guide our design.

As we improved the pan-genotypic activity of our inhibitors, we trended toward improvement of their inhibitory activity against RASs; the structure-activity
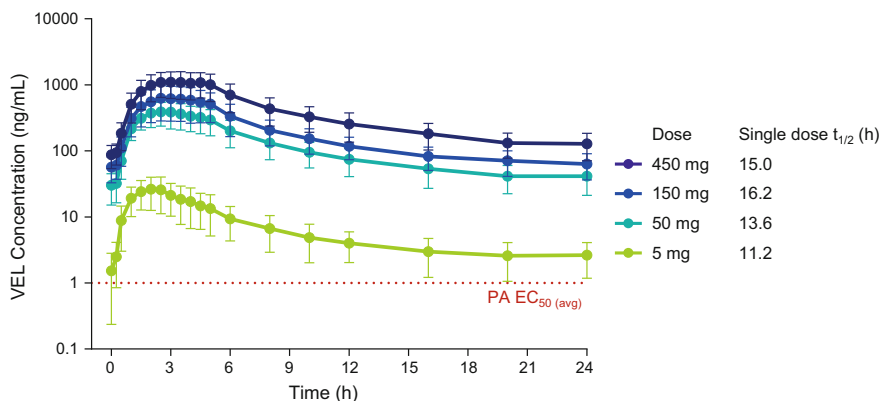
**Fig. 3** VEL PK in healthy volunteers after third daily dose

**Table 14** Ledipasvir and velpatasvir are rulebreakers: bioavailability and "drug-likeness" rule-based metrics

| Rule | Parameter | Rule limit value | LDV value | VEL value |
|------|-----------|------------------|-----------|-----------|
| Lipinski rule of 5 [36] | Molecular weight | ≤500 | 889 | 883 |
| Lipinski rule of 5 | CLogP[a] | ≤5 | 6.71 | 5.70 |
| Lipinski rule of 5 | H-bond donors | ≤5 | 4 | 4 |
| Lipinski rule of 5 | H-bond acceptors[b] (sum N + O) | ≤10 | 14 | 16 |
| Veber [37, 38] | Rotatable bonds[c] | ≤10 | 12 | 13 |
| Veber | Polar surface area[c] | <140 Å | 174 Å | 193 Å |
| Ring rule [33] | # of rings | ≤5 is 95th percentile | 10 | 9 |
| Aromatic ring rule [38] | # aromatic rings | ≤3 | 5 | 6 |

[a]ChemBioDraw 14.0, CambridgeSoft Corporation
[b]Sum of N's and O's as defined by Lipinski et al.
[c]Pipeline pilot

relationships of our various NS5A inhibitors against differing genotypes and their subtypes and RASs are complex. During our discovery of velpatasvir, clinical trial data [39] afforded information regarding GT1 RASs in the NS5A coding region. VEL displays improved replicon potency against a selection of GT1a RASs where LDV shows reduced activity. VEL affords sub-nanomolar activity against all RASs in Table 15 except GT1a Y93H where its $EC_{50}$ is 8.5 nM [1].

As noted (vide supra), we utilized published databases and in-house sequences to identify prevalent sequence variants from patient isolates for non-GT1 sequences. We then generated replicons bearing these variants to determine if they had reduced

**Table 15** LDV and VEL potency against clinically relevant GT1 resistance-associated substitutions (RAS)

| | GT1a EC$_{50}$ (nM) | | | | | | | | GT1b EC$_{50}$ (nM) | |
|---|---|---|---|---|---|---|---|---|---|---|
| | WT | M28T | Q30H | Q30R | L31M | Y93C | Q30E | Y93H | WT | Y93H |
| LDV | 0.031 | 1.9 | 5.7 | 19.6 | 17 | 49.6 | 169 | 52.0 | 0.004 | 7.2 |
| VEL | 0.014 | 0.105 | 0.032 | 0.031 | 0.22 | 0.053 | 0.25 | 8.5 | 0.016 | 0.011 |

All RASs are transiently transfected GT1a or GT1b subgenomic HCV replicons

susceptibility to our inhibitors. Thus we worked to define clinically relevant non-GT1 RASs to guide our NS5A inhibitor discovery process. While a number of these variants that were produced did not exhibit significantly reduced susceptibility to our inhibitors, there were others that did. Table 16 shows the activity of LDV and VEL against a number of these variants that proved challenging to inhibit [1]. These replicons helped guide our discovery process. For example, our selection of VEL for clinical studies was based in part on its high activity against GT3a A30K. Indeed, after initiating clinical studies with VEL, a report of an NS5A inhibitor in combination with sofosbuvir noted relapse with the presence of GT3a A30K virus [40]. VEL is potent with an EC$_{50}$ of 210 pM against GT3a A30K. VEL has improved potency over LDV for all GT2 and GT3 RASs in Table 16.

Velpatasvir produced rapid and sustained viral suppression at all monotherapy dose levels (5–150 mg total dose) in GT1–4-infected individuals [26]. Median viral load reduction (VLR) results versus time for three once-daily oral monotherapy doses (50 or 150 mg) of VEL is plotted in Fig. 4 (three total doses per patient). The VLR for three once-daily oral monotherapy 90 mg doses of LDV (from an independent study) is also plotted in Fig. 4 for reference. The median maximal VLR for each dose is also provided in Fig. 4 [41]. The GT1a median maximal VLR for VEL is 4.2 log10 for both the 50 and 150 mg doses, while it is 3.2 log10 for LDV (90 mg). At all doses the inhibitory quotient (IQ or concentration-fold above the protein adjusted EC$_{50}$ 24 h post-dose, e.g., IQ > 470 for 90 mg LDV, data not shown) for WT virus is very high. The greater VLR for VEL over LDV is a probable consequence of the increased potency of VEL against pre-existing (baseline) RASs (Table 15). A wide range of viral species is present in each patient's sera, and suppression of viral load achieves a maximal value when the drug IQ is insufficient to suppress given RASs that are present in the patient. The pharmacokinetic half-life, WT IQ, and dose are all greater for LDV at the 90 mg dose than for VEL at the 50 mg dose, and therefore it can be seen that these factors are not the drivers of the maximal VLR. VEL encounters viral species with reduced susceptibility prevalent at ~4.2 log10 below baseline, while LDV encounters such species ~3.2 log below baseline. As a further consequence of VEL's potent activity against RASs, VEL maintains nearly maximal suppression of virus in GT1a patients 3 days post the last dose, and in GT1b and GT2 patients, maximal suppression is maintained 5 days post the last dose. GT3 and GT4 patients remain suppressed ~1 and ~1.5 log10 at 5 days post the last dose, respectively (Fig. 4).

**Table 16** LDV and VEL potency against GT2 and GT3 RAS

| | GT2a EC$_{50}$ (nM) | | | | GT2b EC$_{50}$ (nM) | | | | GT3a EC$_{50}$ (nM) | | |
|---|---|---|---|---|---|---|---|---|---|---|---|
| | WT | K44R | N62V | N62S | WT[a](L31M) | WT[b](L31M) | R44K | P58S | WT | A30K | Y93H |
| LDV | 209 | 164 | 222 | 123 | 865 | 211 | 943 | 292 | >44.8 | >88.8 | >88.8 |
| VEL | 0.009 | 0.005 | 0.01 | 0.003 | 0.004 | 0.007 | 0.011 | 0.01 | 0.013 | 0.21 | 3.2 |

GT2a WT is JFH-1 Renilla luciferase (Rluc) subgenomic replicon. GT2a RASs are GT2a backbone which encode the full-length NS5A gene from various GT2a clinical isolates carrying the indicated RAS

GT2b WT are chimeric replicons based on GT2a JFH-1 Rluc subgenomic replicon, encoding the full-length gene from GT2b

GT3a WT is GT3a S52 chimeric replicon based on GT1b Rluc subgenomic replicon backbone. GT3a RASs were produced by site-directed mutagenesis in the WT replicon. ">" indicates the highest concentration tested and EC$_{50}$ was not achieved

[a]MD2b-1 strain or [b]AY232738. GT2b RASs were constructed similarly using GT2b clinical isolates carrying the indicated RAS
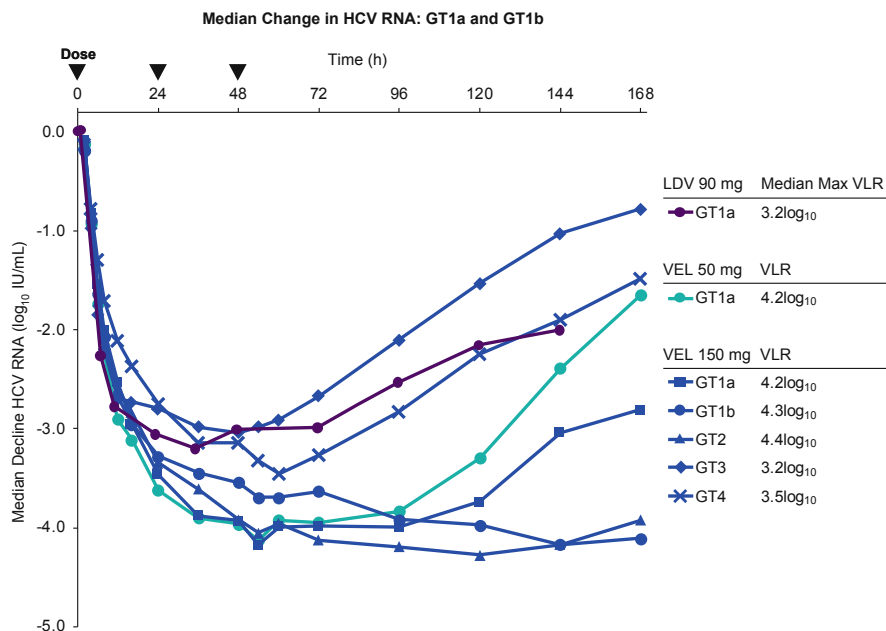
**Fig. 4** Viral load reduction, three daily doses in monotherapy: LDV or VEL. LDV data from a different study

Data points in Fig. 5 depict the maximal viral load attained for each treated GT1a patient in the 5–150 mg cohorts (three once-daily monotherapy doses) [26]. Viral deep sequencing data for GT1a at baseline (prior to treatment, 1% prevalence is the lower limit of detection) are notated in Fig. 5, with some infected individuals displaying extensive pre-existing RASs present at $\geq$1% (limit of detection). All individuals experienced viral load reductions despite the presence of measurable baseline RASs. All RASs assessed in replicons in Table 15 except Q30R are represented in Fig. 5, and the replicon potencies of VEL against GT1a M28T, Q30H, L31M, Y93C, Q30E, and Y93H are all validated through observed viral load reductions in vivo. At the 5 mg dose, the mean maximal VLR was greater than 4 log10, although by happenstance in this cohort no RAS was detected at baseline (1% limit of detection). In contrast one patient in the 50 mg cohort had seven pre-existing RASs, with individual RAS percentages totaling >100%, suggesting that some of these RASs exist at least as double mutants in this patient. Even this individual experienced a >1 log10 viral load reduction.

Maximal VLR are plotted, and the measurable baseline RASs are noted for non-GT1a individual patients in the 150 mg cohort (three once-daily monotherapy doses) in Fig. 6. All individuals with measurable RASs achieved >3 log10 VLR, validating the replicon potency of VEL against GT1b Y93H (>5 log VLR); GT2b L31M (two individuals with >99% prevalence, both >4.5 log10 VLR); and GT3a
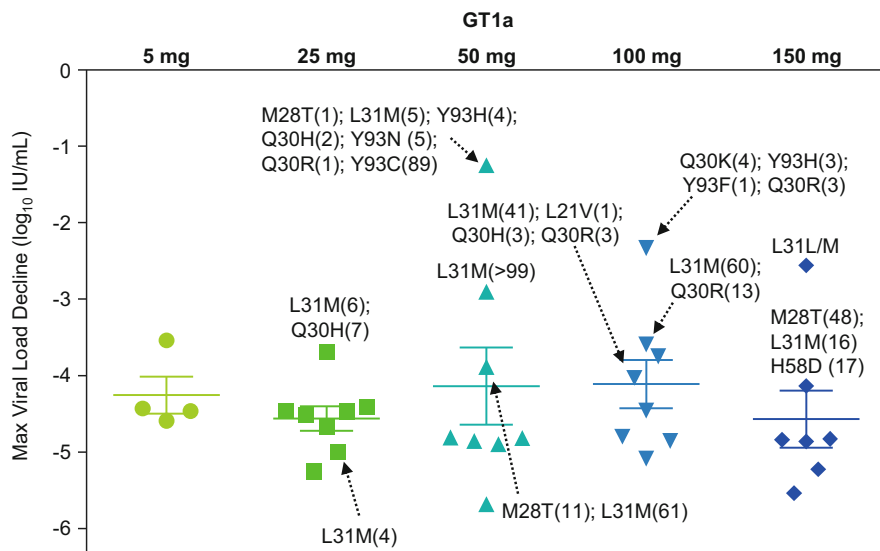
**Fig. 5** GT1a VEL 3-day dosing monotherapy, maximum VLR by individual patient. Mean VLR and standard deviation are provided with the horizontal lines. Individuals with baseline RAS are annotated (measured by deep sequencing, 1% limit of detection) with percent prevalence in parentheses

Y93H and A30K (each >3 log10 VLR). Each of the foregoing RASs is susceptible to VEL in replicon assays in Table 16.

The potent VLR in GT1–4 patients (Fig. 4) and against the wide range of pre-existing GT1–4 RAS in patients (Figs. 5 and 6) validates the replicon assay strategy and inhibitor design approach described herein leading to the discovery of VEL.

# 7   Approval of Epclusa® (SOF/VEL) and Vosevi® (SOF/VEL/VOX)

With velpatasvir we achieved our goal of discovering an NS5A inhibitor with pan-genotypic potency and pharmacokinetics favorable for inclusion in STRs for the treatment of HCV infection. Epclusa® and Vosevi® are the only approved pan-genotypic STRs for the treatment of HCV infection.

In order to simplify therapy, clinical trial design with SOF/VEL focused on defining a single 12-week treatment duration for all patients regardless of genotype, prior treatment experience, cirrhosis status, or the presence of baseline RAS. (A review of the SOF/VEL clinical development can be found in this volume of HCV: The Journey from Discovery to a Cure.) Simplicity of therapy has been achieved with the STR Epclusa® which provides an overall SVR of 98% for
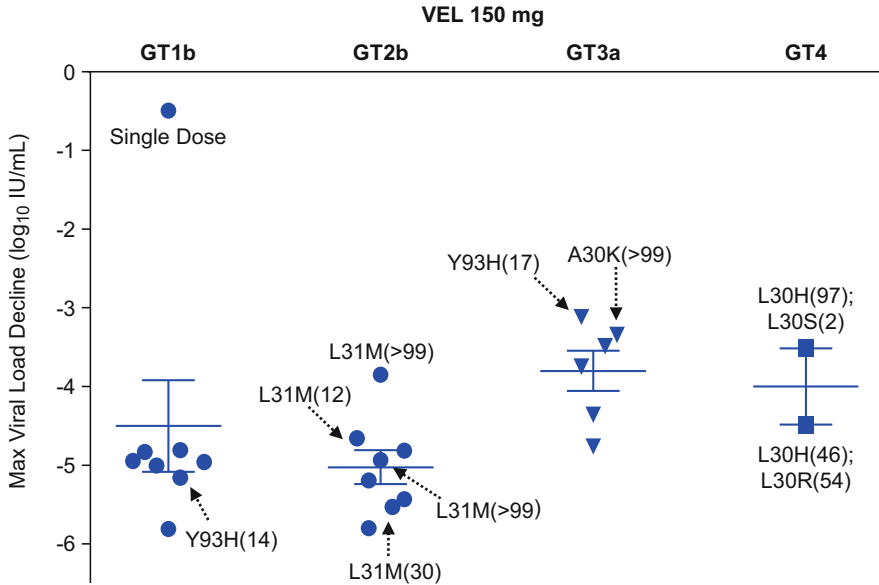
**Fig. 6** GT1–4 VEL 3-day dosing monotherapy, maximum VLR by individual patient. Individuals with baseline RAS noted (measured by deep sequencing) with prevalence in parentheses

GT1–6 patients without cirrhosis or with compensated cirrhosis (ASTRAL Phase 3 clinical trials) [15–19] (https://www.gilead.com/~/media/files/pdfs/medicines/ liver-disease/epclusa/epclusa_pi.pdf. Accessed 24 June 2018). The high SVR rates in the ASTRAL trials were achieved including a wide range of genotypic subtypes: multiple baseline RASs were present in every treatment arm, and 35 subtypes and 13 new or mixed subtypes were represented in these trials. Epclusa® is the first regimen approved for treatment of patients with GT1–6 HCV infection. Epclusa®'s simplification of the HCV treatment landscape upon FDA approval (6/28/16) is apparent in Table 17. Complexities or limitations associated with other approved regimens included contraindication for treatment of some genotypes 1–6; multiple daily pills; twice-daily dosing including differing pill count during day and evening dosing; differing treatment durations (in some cases inclusion of RBV) depending on baseline viral load, presence of baseline RASs, or the presence of compensated cirrhosis; contraindication for the presence of cirrhosis; differing dosages of NS5A inhibitor depending on co-medications (victim drug interactions); and regimen-dependent requirement for pre-treatment testing of HCV genotype, level of cirrhosis, viral load, or baseline RAS (Table 17).

Additionally Vosevi® (SOF 400 mg, VEL 100 mg, VOX 100 mg) has been approved for GT1–6 treatment-experienced patients and affords 96% SVR for patients who failed previous treatment that included an NS5A inhibitor or 98% SVR for patients who failed a treatment not including an NS5A inhibitor (FDA approval July 18, 2017) [20] (https://www.accessdata.fda.gov/drugsatfda_docs/

**Table 17** American Association for the Study of Liver Diseases recommended regimens at the time of SOF/VEL FDA approval

| GT | ±CC | LDV/SOF 10/10/14 | SIM+SOF 11/5/14 | PTV/RTV/OBV+DSV 12/19/14 | PTV/RTV/OBV+DSV+RBV 12/19/14 | PTV/RTV/OBV+RBV 7/24/15 | DCV+SOF 7/24/15 | EBR/GZB 1/28/16 | SOF/VEL 6/28/16 |
|---|---|---|---|---|---|---|---|---|---|
| 1a | − | 8 or 12 weeks | 12 | | 12 | | 12 (30/60/90 mg)[a] | 12 or 16+RBV (12 if no RAS) | 12 |
| 1a | + | 12 weeks | | | | | | 12 or 16+RBV (12 if no RAS) | 12 |
| 1b | − | 8 or 12 | 12 | 12 | | | 12 (30/60/90 mg)[a] | 12 | 12 |
| 1b | + | 12 | | 12 | | | | 12 | 12 |
| 2 | − | | | | | | | | 12 |
| 2 | + | | | | | | | | 12 |
| 3 | − | | | | | | 12 (30/60/90 mg)[a] | | 12 |
| 3 | + | | | | | | 24[a] ± RBV | | 12 |
| 4 | − | 12 | | | | 12 | | 12 | 12 |
| 4 | + | 12 | | | | | | 12 | 12 |
| 5 | − | 12 | | | | | | | 12 |
| 5 | + | 12 | | | | | | | 12 |
| 6 | − | 12 | | | | | | | 12 |
| 6 | + | 12 | | | | | | | 12 |

Nucleotide NS5A Protease NS5B RBV PK Booster ☀☾ Morning and evening dose if 2x daily ● 1 pill ▨ Not recommended ▨ Recommended

Number in green box represents treatment time in weeks

LDV/SOF 8 weeks for patients with VL < 6 million IU. EBR/GZB GT1a pre-treatment NS5A RAS testing is recommended

Date corresponds to the first FDA approval for each drug combination (some combinations added further indications at later dates)

[a]DCV dose depends on victim drug interactions with certain co-dosed HIV drugs

+CC compensated cirrhosis, −CC non-cirrhotic, DCV daclatasvir, DSV dasabuvir, EBR elbasvir, GZB grazoprevir, OBV ombitasvir, PTV paritaprevir, RBV ribavirin, RTV ritonavir, SIM simeprevir

label/2017/209195s000lbl.pdf. Accessed 10 June 2018); Vosevi® is also approved for 8-week therapy in GT1–6 treatment-naïve patients affording 95% SVR [21] (European Medicines Agency).

# 8 Epclusa® (Sofosbuvir/Velpatasvir) Real-World Effectiveness

The real-world effectiveness [42, 43] comparing Harvoni® (LDV 90 mg, SOF 400 mg) to the earlier IFN-based standard of care is discussed in the ledipasvir discovery chapter in this volume and represented a major advance for the treatment

of patients with HCV infection. Real-world SVR rates for IFN-based therapy are as low as 3% reflecting the complexity, toxicity, and poor efficacy of these regimens, and IFN-based regimens are therefore untenable for widespread therapeutic use [13]. In contrast, Harvoni affords real-world SVR rates comparable to the $\geq$95% SVR achieved in controlled clinical trial settings [44] and accordingly has played a major role in the eradication of the virus within the 200,000 US veteran's administration HCV-infected patients, with eradication targeted for the end of 2018 [45].

Simplification of therapy has further advanced with the safety and efficacy of the pan-genotypic Epclusa® 12-week regimen and translates to high cure rates in real-world settings (Table 18). In three real-world efficacy studies, Epclusa® afforded high SVR rates: 97% (91/94 GT2 patients and 66/68 GT3 patients; TRIO network) [46] and 99.5% (213/214 GT3 patients, German hepatitis C cohort [GECCO]) [19]. The results from the GECCO study are even more striking considering that GT3 infection had been considered the most difficult genotype to cure early in the DAA era [47].

Epclusa®'s practicality as a pan-genotypic single duration treatment regimen has been applied to a minimal monitoring study with no on-treatment study assessments in a resource-limited setting. Broad enrollment criteria allowed inclusion of patients

**Table 18** SOF/VEL or SOF/VEL/VOX clinical trial (Phase III) and real-world effectiveness SVR results

| Study | GT | Study characteristics | Overall SVR% | |
|---|---|---|---|---|
| ASTRAL-1 | 1, 2, 4–6 | Treatment-naïve/treatment-experienced cirrhotic and non-cirrhotic | 99% | (618/624) |
| ASTRAL-2 | 2 | Treatment-naïve/treatment-experienced cirrhotic and non-cirrhotic | 99% | (133/134) |
| ASTRAL-3 | 3 | Treatment-naïve/treatment-experienced cirrhotic and non-cirrhotic | 95% | (264/277) |
| ASTRAL-4 | 1–4 | Decompensated cirrhosis | 83% | (75/90) |
| ASTRAL-5 | 1–4 | HIV/HCV coinfected; treatment-naïve/treatment-experienced cirrhotic and non-cirrhotic | 95% | (99/104) |
| Trio GT2 | 2 | Real-world effectiveness | 97% | (91/94) |
| Trio GT3 | 3 | Real-world effectiveness | 97% | (66/68) |
| GECCO | 3 | Real-world effectiveness | 99.5% | (213/214) |
| POLARIS-1 | 1–6 | NS5A-experienced | 96% | (253/263) |
| POLARIS-2 | 1–6 | 8 week, DAA-naïve, 18% with cirrhosis | 95% | (477/501) |
| POLARIS-3 | 3 | 8 week, DAA-naïve, 100% with cirrhosis | 96% | (106/110) |
| POLARIS-4 | 1–6 | DAA-experienced, no NS5A | 98% | (178/182) |

ASTRAL and POLARIS are Phase III clinical trials
SOF/VEL/VOX in POLARIS 1–4. All others are SOF/VEL

with any HCV genotype, with or without cirrhosis, and with treatment status as naïve or experienced. The overall SVR rate was 93% (including five patients lost to follow-up and one who withdrew consent) and 97.5% when based on virologic failure in this study in India [48].

## 9    Conclusion

The treatment of HCV-infected individuals with direct-acting antivirals represents the first time that a widespread, life-threatening chronic disease can be cured. The simple, safe, and effective pan-genotypic STRs Epclusa® and Vosevi® provide a means for broad treatment and cure of HCV-infected individuals worldwide.

**Compliance with Ethical Standards**

**Conflict of Interest**: John O. Link is an employee of Gilead Sciences, Inc.

**Ethical approval**: All procedures performed in the studies involving human participants were in accordance with the ethical standards of the institutional and/or national research committee and with the 1964 Helsinki declaration and its later amendments or comparable ethical standards.

**Informed Consent**: Informed consent was obtained from all individual participants included in the study.

## References

1. Cheng G., Yu M., Peng B., Lee Y.-J., Trejo-Martin A., Gong R., Bush C., Worth A., Nash M., Chan K., Yang H., Beran R., Tian Y., Perry J., Taylor J., Yang C., Paulson M., Delaney W., Link J. O. (2013) J Hepatol 58(Suppl):S484. http://www.natap.org/2013/EASL/EASL_34.htm. Accessed 10 June 2018
2. Link JO, Taylor JG, Xu L, Mitchell M, Guo H, Liu H, Kato D, Kirschberg T, Sun J, Squires N, Parrish J, Keller T, Yang ZY, Yang C, Matles M, Wang Y, Wang K, Cheng G, Tian Y, Mogalian E, Mondou E, Cornpropst M, Perry J, Desai MC (2014). J Med Chem 57:2033
3. Guo H, Kato D, Kirschberg TA, Liu H, Link JO, Mitchell ML, Parrish JP, Squires N, Sun J, Taylor J, Bacon EM, Canales E, Cho A, Cottel JJ, Desai M, Halcomb RL, Krygowski ES, Lazerwith SE, Mackman R, Pyun HJ, Saugier JH, Trenkle J, Tse W, Vivian RW, Schroeder SD, Watkins WJ, Xu L, Yang Z-Y, Kellar T, Sheng X, Clarke M, O'Neil H, Chou C-H, Graupe M, Jin H, McFadden R, Mish M, Metobo R, Phillips BW, Venkataramani C (2010) Patent Application. WO 2010/132601 A1
4. Porter DP, Guyer B (2013) In: Desai MC, Meanwell NA (eds) Successful strategies for the discovery of antiviral drugs. The Royal Society of Chemistry, Cambridge, p 482

5. Blanco JL, Montaner JS, Marconi VC, Santoro MM, Campos-Loza AE, Shafer RW, Miller MD, Paredes R, Harrigan R, Nguyen ML, Perno CF, Gonzalez-Hernandez LA, Gatell JM (2014). AIDS 28:2531–2539

6. Sofia MJ, Link JO (2017) In: Chackalamannil S, Rotella D, Ward S (eds) Comprehensive medicinal chemistry III. Elsevier, Amsterdam, p 558

7. Petruzziello A, Marigliano S, Loquercio G, Cozzolino A, Cacciapuoti C (2016). World J Gastroenterol 22:7824

8. Strader DB, Seeff LB (2012). Clin Liver Dis 1:6

9. Hoofnagle JH, Seeff LB (2006). N Engl J Med 355:2444

10. Moon AM, Green PK, Berry K, Ioannou GN (2017). Aliment Pharmacol Ther 45:1201–1212

11. Link JO, Taylor JG, Trejo-Martin TA, Kato D, Katana AA, Krygowski ES, Yang Z-Y, Zipfel S, Cottell JJ, Bacon EM, Tran CV, Yang CY, Wang Y, Wang K, Zhao G, Cheng G, Tian Y, Gong R, Lee J, Yu M, Gorman E, Mogalian E, Perry J. Bioorg Med Chem Lett. Submitted

12. Link JO (2018). Med Chem Rev 53:541–564

13. North CS, Hong BA, Adewuyi SA, Pollio DE, Jain MK, Devereaux R, Quartey NA, Ashitey S, Lee WM, Lisker-Melman M (2012). Gen Hosp Psychiatry 35:122

14. Sofia M (2015). J Med Chem Rev 50:397

15. Feld JJ, Jacobson IM, Hezode C, Asselah T, Ruane PJ, Gruener N, Abergel A, Mangia A, Lai CL, Chan HL, Mazzotta F, Moreno C, Yoshida E, Shafran SD, Towner WJ, Tran TT, McNally J, Osinusi A, Svarovskaia E, Zhu Y, Brainard DM, McHutchison JG, Agarwal K, Zeuzem SN (2015). Engl J Med 373:2599

16. Foster GR, Afdhal N, Roberts SK, Brau N, Gane EJ, Pianko S, Lawitz E, Thompson A, Shiffman ML, Cooper WJ, Towner WJ, Conway B, Ruane P, Bourliere M, Asselah T, Berg T, Zeuzem S, Rosenberg W, Agarwal K, Stedman CA, Mo H, Dvory-Sobol H, Han L, Wang J, McNally J, Osinusi A, Brainard DM, McHuchison JG, Mazzotta F, Tran TT, Gordan SC, Patel K, Reau N, Mangia A, Sulkowski M (2015). N Engl J Med 373:2608

17. Curry MP, O'Leary JG, Bzowej N, Muir AJ, Korenblat KM, Fenkel JM, Reddy KR, Lawitz E, Flamm SL, Schiano T, Teperman L, Fontana R, Schiff E, Fried M, Doehle B, An D, McNally J, Osinusi A, Brainard DM, McHutchison JG, Brown Jr RS, Charlton M (2015). N Engl J Med 373:2618

18. Wyles D, Bräu N, Kottilil S, Daar ES, Ruane P, Workowski K, Luetkemeyer A, Adeyemi O, Kim AY, Doehle B, Huang KC, Mogalian E, Osinusi A, McNally J, Brainard DM, McHutchison JG, Naggie S, Sulkowski M (2017). Clin Infect Dis 65:6

19. von Felden J, Vermehren J, Ingiliz P, Mauss S, Lutz T, Simon KG, Busch HW, Baumgarten A, Schewe K, Hueppe D, Boesecke C, Rockstroh JK, Daeumer M, Luebke N, Timm J, Schulze Zur Wiesch J, Sarrazin C, Christensen S (2018). Aliment Pharmacol Ther 47:1288

20. Taylor JG, Zipfel S, Ramey K, Vivian R, Schrier A, Karki KK, Katana A, Kato D, Kobayashi T, Martinez R, Sangi M, Siegel D, Tran CV, Yang Z-Y, Zablocki J, Yang CY, Wang Y, Wang K, Chan K, Barauskas O, Cheng G, Jin D, Schultz B, Appleby T, Villasenor A, Link JO. Bioorg Med Chem Lett. Submitted

21. Jacobson IM et al (2017). Gastroenterology 153:113–122

22. Torres-Puente M, Cuevas JM, Jimenez-Hernandez N, Bracho MA, Garcia-Robles I, Wrobel B, Carnicer F, Del Olmo J, Ortega E, Moya A, Gonzalez-Candelas F (2008). J Viral Hepat 15:188

23. Nguyen T, Guedj J (2015). CPT Pharmacometrics Syst Pharmacol 4:231

24. Macdonald A, Harris M (2004). J Gen Virol 85:2485–2502

25. Scheel TK, Gottwein JM, Mikkelsen LS, Jensen TB, Bukh J (2011). Gastroenterology 140:1032

26. Lawitz EJ, Dvory-Sobol H, Doehle BP, Worth AS, McNally J, Brainard DM, Link JO, Miller MD, Mo H (2016). Antimicrob Agents Chemother 60:5368

27. Bilello JP, Lallos LB, McCarville JF, La Colla M, Serra I, Chapron JM, Pierra C, Sandring DN, Seifer M (2014). Antimicrob Agents Chemother 58:4431–4442

28. Bacon EM, Cottell JJ, Katana AA, Kato D, Krygowski ES, Link JO, Taylor J, Tran CV, Trejo-Martin TA, Yang Z-Y, Zipfel S (2012) Patent application. WO 2012/068234 A2

29. Bacon EM, Cottell JJ, Katana AA, Kato D, Krygowski ES, Link JO, Taylor J, Tran CV, Trejo-Martin TA, Yang Z-Y, Zipfel S (2013) Patent application. WO 2013/075029
30. Doak BC, Over B, Giordanetto F, Kihlberg J (2014). Chem Biol 21:1115
31. Rowland M, Tozer TN (2011) Clinical pharmacokinetics and pharmacodynamics: concepts and applications, 4th edn. Wolters Kluwer Health/Lippincott William & Wilkins, Philadelphia
32. He YL, Murby S, Warhurst G, Gifford L, Walker D, Ayrton J, Eastmond R, Rowland M (1998). J Pharm Sci 87:626
33. Taylor RD, MacCoss M, Lawson AD (2014). J Med Chem 57:5845
34. Lipkus AH, Yuan Q, Lucas KA, Funk SA, Bartelt 3rd WF, Schenck RJ, Trippe AJJ (2008). Org Chem 73:4443–4451
35. Mogalian E, German P, Kearney BP, Yang CY, Brainard D, Link J, McNally J, Han L, Ling J, Mathias A (2017). Antimicrob Agents Chemother 61:1
36. Lipinski CA, Lombardo F, Dominy BW, Feeney P (1997). J Adv Drug Deliv Rev 23:3
37. Veber DF, Johnson SR, Cheng HY, Smith BR, Ward KW, Kopple KD (2002). J Med Chem 45:2615
38. Ritchie TJ, Macdonald S (2009). J Drug Discov Today 14:1011
39. Wong KA, Worth A, Martin R, Svarovskaia E, Brainard DM, Lawitz E, Miller MD, Mo H (2013). Antimicrob Agents Chemother 57(12):6333–6340
40. Sulkowski MS, Gardiner DF, Rodriguez-Torres M, Reddy KR, Hassanein T, Jacobson I, Lawitz E, Lok AS, Hinestrosa F, Thuluvath PJ, Schwartz H, Nelson DR, Everson GT, Eley T, Wind-Rotolo M, Huang S-P, Gao M, Hernandez D, McPhee F, Sherman D, Hindes R, Symonds W, Pasquinelli C, Grasela DM (2014). N Engl J Med 370:211
41. Lawitz EJ, Gruener D, Hill JM, Marbury T, Moorehead L, Mathias A, Cheng G, Link JO, Wong KA, Mo H, McHutchison JG, Brainard DM (2012). J Hepatol 57:24
42. Singal AG, Higgins PD, Waljee AK (2014). Clin Transl Gastroenterol 5:e45
43. Nordon C, Karcher H, Groenwold RH, Ankarfeldt MZ, Pichler F, Chevrou-Severac H, Rossignol M, Abbe A, Abenhaim L, On behalf of the GetReal Consortium (2016). Value Health 19:75
44. Backus LI, Belperio PS, Shahoumian TA, Loomis TP, Mole LA (2016). Hepatology 64:405–414
45. US Medicine. http://www.usmedicine.com/agencies/department-of-veterans-affairs/va-could-soon-achieve-near-complete-eradication-of-hepatitis-c/. Accessed 16 June 2018
46. Conference reports for NATAP. http://natap.org/2017/EASL/EASL_24.htm%20. Accessed 23 Dec 2018
47. Ampuero J, Romero-Gomez M, Reddy KR (2014). Aliment Pharmacol Ther 39:686
48. Sood A, Duseja A, Kabrawala M, Amrose P, Goswami B, Chowdhury A, Sarin SK, Koshy A, Hyland RH, McNabb B, Lu S, Camus G, Stamm LM, Brainard DM, Subramanian GM, Prasad M, Gupta S, Kumar S, Bhatia S, Shah SR, Kapoor D, Shalimar, Saraswat V (2018) Asian Pacific Association for The Study of the Liver (APASL), New Delhi, India, O-HCV-12